Journal of Materials Chemistry B

Accepted Manuscript

ROYAL SOCIETY OF CHEMISTRY

www.rsc.org/materialsB

Journal of Materials Chemistry B

ARTICLE

Tough and Fully Recoverable Hydrogels

Junhua Wei[a], Jilong Wang[a], Siheng Su[a], Shiren Wang[b]*, and Jingjing Qiu[a]*

Received 00th January 20xx,
Accepted 00th January 20xx

DOI: 10.1039/x0xx00000x

www.rsc.org/

In the natural cartilage, collagen fibers form the extracellular matrix while the aggrecan entangle with these fibers and provides cartilage with its osmotic properties, which are critical to resist cyclic compressive loads. In this paper, a hydrogel was fabricated through entanglement of a bio-inspired nanostructure (Chondroitin Sulfate coated Vinyl Silica nanoparticles, CS-SNP) within agar/Poly (acrylamide) double network hydrogel. The highly charged chondroitin sulfate groups provide additional compression resistance support within macromolecular chains while the solid silica cores anchor these entanglements. The presence of the CS-SNP not only improved the compressive modulus, compressive strength, fracture toughness, and fatigue resistance of this hydrogel, but also ensured the full recovery of all these properties after thermal heating. This tough, fully recoverable, and robust hydrogel is a promising material for applications with strong mechanical requirements.

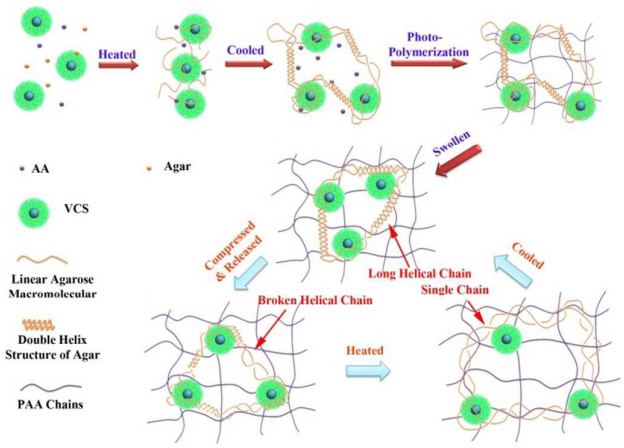

1. Introduction

Hydrogels are being developed for variable applications, including tissue engineering, drug delivery, and even robot[1-6]. However, the weak and brittle traditional hydrogel cannot afford the potential applications with mechanical requirements. Although strong and tough hydrogels have been studied for decades and great advances have been made in the recent years to develop tough hydrogel structures, such as slide-ring, triblock copolymers, tetra-PEG gels, and macromolecular microsphere composite hydrogels[7-9], their time-consuming multi-step synthesis/polymerization, low mechanical performance, and the failure after cyclic loading significantly hinder their applications.

The emerging double network hydrogel (DN gel) with excellent elastic modulus (0.1-1.0 MPa), tensile strength (tensile fracture stress: 1-10 MPa), tensile resiliency (tensile fracture strain: 1000-2000%), compressive fracture stress (20-60 MPa), and notched fracture toughness (tearing energy: 100-4500 J/m^2) has drawn significant attentions recently[10-13]. This is because its simple design allowing the usage of biopolymers, including agar[14], bacterial cellulose[15], gellan gum[16], and sodium alginate[7]. However, its poor fatigue resistant due to its special network structure[17] and the lack of the recovery mechanism restrict its applications. In the DN gel, a densely crosslinked rigid network (the N1 network) withstands energy dissipation during loading and a sparsely crosslinked ductile network (the N2 network) keeps its integration[18, 19]. When suffering force, the first network absorbs and dissipates the energy while the second network maintains the shape. After the loading, the mechanical properties of DN gels dramatically decreased (~ 50%)[20] because of the scarification of first networks. The poor fatigue resistance make the DN gel more vulnerable than other tough hydrogel structures to cyclical loading. In order to solve this problem, thermoreversible sol-gel polysaccharide/poly (acrylamide) hydrogels [14, 21] with high mechanical performance and recoverable functionality were reported. After the sol-gel transition of the first network at a certain temperature, the N1 network is reformed and the mechanical properties of the hydrogel are partially recovered. However, there are still two problems with this structure: (1) poor hardness (~123 kPa[14]). That's to say, the thermoreversible hydrogel is too soft to provide sufficient mechanical support within a small range of strain. (2) Partial fracture toughness recovery (65%[14]) since the broken and uncharged first network cannot be fully restored

[a] Department of Mechanical Engineering, Texas Tech University, Box 41021, Lubbock TX 79409, Tel: (806)834-8076, Email: Jenny.Qiu@ttu.edu
[b] Department of Industrial and Systems Engineering, Texas A&M University, College Station, TX 77843-3131, Tel: (979)458-2357, Email: S.wang@tamu.edu
DOI: 10.1039/x0xx00000x

to the original and uniform density. Its ability to dissipate energy decayed rapidly during compressive cycles. Enhancing the mechanical properties and improving the recovery ratio of the polysaccharide DN gels is demanded.

Aggrecan, one of the major components of cartilage, exhibits a bottlebrush structure in which chondroitin sulfate (CS) is anchored onto an extended protein core [22]. Because the high osmotic pressure provided by its highly charged CS side chains, aggrecan is considered to be the key structure to resist compressive loading within the cartilage [23]. The previous research has also proved the modulus and tensile strength of a DN gel are increased by 370% and 400%, respectively with addition of 0.82 wt% aggrecan[24]. Therefore, the addition of aggrecan is a promising way to enhance compressive modulus and maintain a more stable microstructure of thermoreversible sol-gel polysaccharide/poly (acrylamide) hydrogel. However, the natural aggrecan is difficult to extract and the synthesis of aggrecan mimic is time consuming due to the complicated processing and the strict reaction conditions [25]. It is anticipated that a bio-inspired structure with easy processabilty can be mass produced and used to enhance the osmotic pressure inside the thermoreversible hybrid gel systems.

In this work, aggrecan-mimic highly charged nanoparticles were fabricated by anchoring chondroitin sulfate functional groups onto vinyl modified silica nanoparticle (VSNP) to form chondroitin sulfate coated silica nanoparticles (CS-SNP). The large surface-to-volume specific surface and abundant vinyl groups on the silica nanoparticle enable the conjugation of a large amount of chondroitin sulfate chains. The existence of CS-SNP in the hybrid gel system provided significantly enhanced osmotic pressure, which can enhance mechanical properties of the DN gel like aggrecan in natural cartilage. In addition, the entanglement of the CS-SNP with thermal-reversible sol-gel polysaccharide can support polysaccharide to have uniform dispersion within PAA (polyacrylamide) network after large loading due to their electrostatic interaction which is benefit to improve its recovery rate. This CS-SNP enhanced agar/PAA artificial scaffold with high mechanical performances and fully recoverable mechanism is promising to extend the application areas of hydrogels.

2. Materials and Methods

2.1 Materials

Chondroitin sulfate, tetraethoxysilane (TEOS), vinyltriethoxysilane (VTEOS), ammonium hydroxide solution (NH_4OH), sodium borate buffer, EtOH, allyl glycidyl ether (AGE), acrylamide (AA), N,N'- methylenebis (acrylamide) (MBAA), agar, Irgacure 2959, and ammonium persulfate (APS) were purchased from Sigma Aldrich.

2.2 Allyl Glycidyl Ether Functionalized Chondroitin Sulfate (AGE-CS)

In order to attach highly charged CS groups to silica based nanoparticles, AGE was firstly used to conjugate double bonds to CS through its amine groups. AGE, an epoxide and vinyl containing monomer, can react with amine groups at an alkaline condition. AGE was added into 10 mg/ml CS in sodium borate buffer (SBB, 0.1M, pH 9.4) to form a 1000:1 molar ratio of AGE to CS [26, 27]. After stirring this solution for 24 hrs, the AGE functionalized CS (AGE-CS) was purified by dialysis (12kDa MWCO dialysis membrane) for 7 days. The concentration of the purified AGE-CS solution was adjusted to 10 mg/ml. The attachment of AGE on CS was confirmed by FTIR spectrum (Fourier-Transform Infrared, Nicolet iS10).

2.3 Vinyl Modified Silica Nanoparticles (VSNP)

0.9 M NH_4OH and 9.5 M water were added in 100 ml of EtOH (200 proof). When this solution was heated to 40 ^{o}C, a 1:1 (w/w) solution of TEOS (0.25 M) in EtOH was added suddenly with vigorous stirring. After 5 min of stirring, VTEOS (TEOS/VTEOS molar ratio is 85:15) was added when the reaction mixture started to become turbid. After 30 min of stirring, the white precipitates were collected by centrifugation at 5000 rpm for 30 min and then washed with water and EtOH repetitively [28]. The morphologies of SNP and VSNP were investigated by TEM (Transmission Electron Microscopy, HITACHI T8100). The surface functional groups and composition were studied by FTIR and TGA (Thermogravimetric Analyzer, TA Q50).

2.4 Chondroitin Sulfate Coated Vinyl modified Silica Nanoparticles (CS-SNP)

The chondroitin sulfate coated silica nanoparticles were prepared by free radical reaction through the vinyl groups. After sonicating 5 ml of 1mg/ml VSNP solution for 30 min, 100 ml of the 10 mg/ml purified AGE-CS solution was added. After bubbling the mixture by nitrogen gas for 15 min, 5 mg of APS was added. The mixture was stirred, heated at 65 ^{o}C and protected by the nitrogen atmosphere for 10 hrs. The unreacted VSNP was removed from the solution by vacuum filtration through a 220-nm membrane and the CS-SNP particles were collected after high-speed centrifugation (14000 rpm) which ensured the precipitation of the less soluble CS-SNP. The fabrication process is illustrated in Fig. 1.

2.6 Double Network Hydrogel

The CS-SNP enhanced double network hydrogel (CS-DN gel) was synthesized using CS-SNP solution. 200 mg of agar, 4 M AA, 0.03 mol% MBAA and 1 mol% photoinitiator (Irgacure 2959) was dispersed in 10 ml of CS-SNP solution (4 mg/ml, 1.5 wt% to the polymer weight). After bubbled with nitrogen gas for 15 min, the solution was heated up to 90 ^{o}C in an oil bath. The transparent solution was then injected into a Teflon mold to fabricate a 5 mm thick and 5 mm diameter cylinder hydrogel. After stored in the refrigerator for 10 hr, the mold was transferred to a glove box protected by nitrogen gas and the CS-DN gel was prepared after 1-hr of irradiation at 365 nm using a 5 watt UV lamp. The control sample, pristine double network, (DN gel), was prepared using DI water instead of the CS-SNP solution. After the fabrication, the as-prepared DN gel was immerged in a large amount of DI water for 24 hrs for swollen samples.

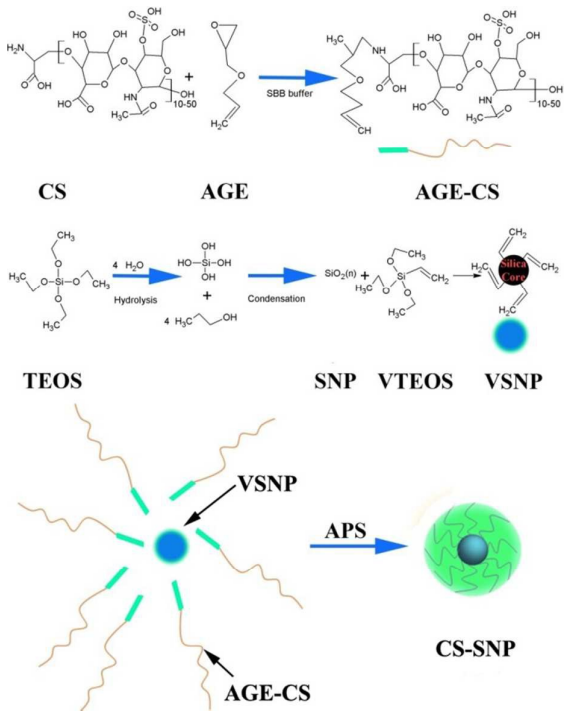

Fig. 1. The scheme of fabricating Chondroitin Sulfate coated Vinyl modified Silica Particles (CS-SNP).

The microstructures of hydrogel samples were imaged by SEM after freeze-drying at -20 °C for 4 days (Scanning Electron Microscope, HITACHI S4300). The mechanical properties of the hydrogels were investigated by unconfined uniaxial compressive measurements (SHMADZU, AGS-X) on hydrogel cylinder at 10% strain per min speed.

The effects of thermal-recoverable on the mechanical properties of the hydrogels were studied. After the compression reached the 99% strain and the load was released, the hydrogel samples were heated for 5 min at 90 °C and then cooled in refrigerator for 1 hr before the subsequent compressive measurement. The fracture toughness of each cycle was compared to the fracture toughness of the first compression to calculate the recovery rate.

The fatigue resistance of the DN and CS-DN is analysed by consecutive loading-unloading test with gradually increasing compressive strain from 30%, 60%, to 90%. At each strain, 5 successive cycles were tested.

The nominal compressive stress (σ_{nom}) was calculated as σ=Load/πR^2, where R is the radius of the cylindrical specimen. The true compressive stress ($\sigma_{true}=\lambda\ \sigma_{nom}$) [29], which are the forces per cross-sectional area, was used to determine the fracture stress and strain, while λ is the deformation ratio ($\lambda = h/h_0$, h_0 is the original thickness of cylinder gel, h is its current thickness.). The strain (ε) is calculated as $\varepsilon=100\%\times(h_0-h)/h_0$. Stress and Strain between ε =0 to 0.1 were used to calculate the elastic modulus (E).

The toughness is defined as:

$$\gamma = \frac{\int_0^{\varepsilon_f} \mathrm{Fds}}{\pi R^2} \qquad (1)$$

where F is the loading, ε_f is the facture stress, and s is the displacement to the corresponding strain.

The strain work to 30% is defined as:

$$U_{30\%} = \frac{\int_0^{0.3_{loading}} \mathrm{Fds} - \int_0^{0.3_{unloading}} \mathrm{Fds}}{\pi R^2} \qquad (2)$$

The $U_{30\%}$ represents the energy applied on the hydrogel to achieve 30% compressive strain.

The swelling test is implanted by submerging gels into large amount of DI water at room temperature. The swelling ratio was calculated as $Swelling\ Ratio = (W_t - W_o) \times 100\%$, where W_o is the weight of gel before submerging and W_t is the weight of gel at time t.

For all tests, 5 replicates were tested.

3. Results and Discussion

3.1 Material Characterization of AGE-CS

The synthesized AGE-CS was investigated by the FTIR spectra in Fig. 2. The CS contains: S=O (1230 cm^{-1}), C-O-S (812, 927, 730 cm^{-1}), -OH (3200-3600 cm^{-1}), amide/carboxyl (1621 cm^{-1}), C-C (1130 cm^{-1}), C-H (1550 cm^{-1} and 2861 cm^{-1}), and C-O (1052 cm^{-1}) [30, 31]. The shoulder peaks at 912 cm^{-1} (epoxide), 1094 cm^{-1} (ether stretching, -O-), 2857 cm^{-1} (CH2=CH2 stretching), and 1647 cm^{-1} (alkyl stretching, -CH3) on the AGE-CS validated the successful functionalization of AGE onto CS [26, 32].

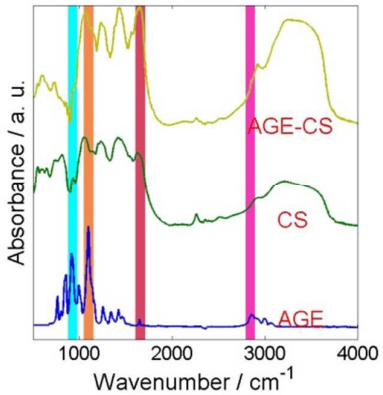

Fig. 2. The FTIR spectra of AGE, CS, and AGE-CS.

3.2 Material Characterization of VSNP

VSNP nanoparticles were firstly tested by the FTIR spectra (Fig. 3 (a)). The FTIR spectrum of pristine silica nanoparticles (SNP) presents peaks at 1050, 950, and 800 cm^{-1}, which are attributed to Si-O-Si, Si-OH, and Si-O-Si, respectively. In comparison, the peaks at 1410 cm^{-1} (=CH2) and 1635 cm^{-1} (C=C) on the FTIR spectrum of VSNP indicate the existence of double bonds [33, 34]. The TGA results (Fig. 3 (b)) further confirmed the existence of the thermally unstable double bonds on the surface of VSNP nanoparticles as there is a larger weight loss around 600°C for the VSNP sample. The TEM images in Fig. 3(c) and (d) indicated the average sizes of SNP and VSNP to be about 150-200nm. The TEM images also demonstrated the different surface morphologies for SNP and VSNP due to the existence of vinyl shells on the smooth surface of silica nanoparticles. All the FTIR, TGA, and TEM

results indicate that the double bond has been integrated onto silica nanoparticles.

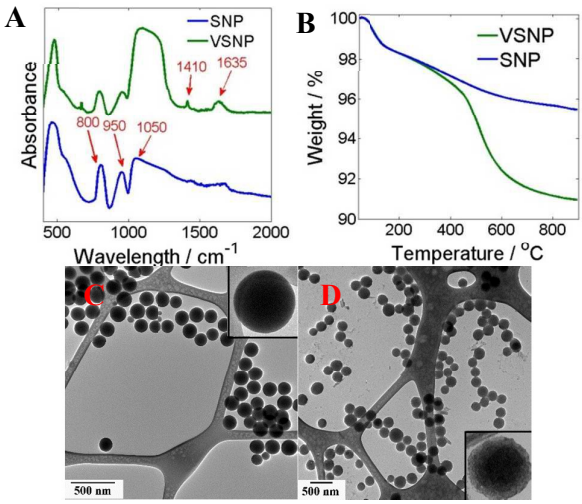

Fig. 3. The FTIR (a) and TGA (b) results of SNP and VSDN. The TEM images of SNP (c) and VSNP (d);

3.3 Chondroitin Sulfate coated Vinyl modified Silica Nanoparticles

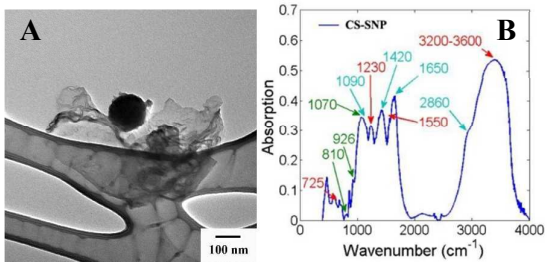

Fig. 4. The TEM image (a) and FTIR spectra (b) of CS-SNP.

The attachment of the CS onto SNP is verified by TEM images and FTIR spectrum. The CS chains were observed to be attached on the SNP core, as seen in Fig. 4(a). The spread of the CS chains results from the charge repelling between CS chains makes the CS-SNP a micrometer sized structure. The FTIR spectrum also confirmed the attachment of CS on the SNP (Fig. 4(b)). The peaks at 725, 1230, 1550, 2861 and 3200-3600 cm^{-1} represent the C-O-S, S=O, C-H, -C-H and -OH groups in the CS; the peaks at 1090 and 1650 cm^{-1} represents the -O- and -CH_3 groups in the AGE; and the peaks at 810, 926, and 1070 cm^{-1} represents Si-O-Si, Si-OH, and Si-O-Si groups in the SNP, respectively. The vanishing of the peak at 1410 cm^{-1} and the shoulder peak at 2857 cm^{-1} indicated the full reaction of the double bond.

The SNP was used as the core to anchor CS chains. The vinyl groups on the SNP provide enough reaction sites for CS so that a great amount of CS groups can be attached to the surface of SNP and spread out to provide large-surface-area negative charge around the nanoparticles.

3.4 Mechanical Properties of Hydrogel

Although the strength of as-prepared agar/PAA DN gel is as strong as natural load-bearing tissues, its application is restricted because of its rough surface, which can't provide a low friction surface to efficiently reduce stress during loading. Fig. 5 shows the picture of an as-prepared CS-DN gel during slicing resistance tests. Although the structure of the as-prepared CS-DN gel didn't break, there are several macroscopic cracks on the surface after the slicing. Compared with the as-prepared CS-DN, there is no crack on the swollen CS-DN after the slicing resistance test which indicated better structure integration. The sol contents of the as-prepared DN and CS-DN are measured to be 89.03 ±5.04% and 95.95 ±1.63%, respectively.

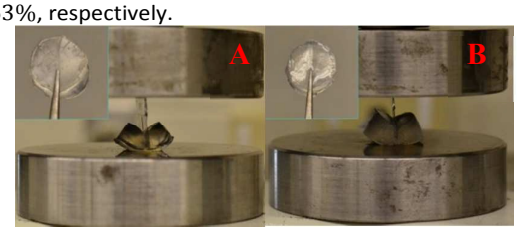

Fig. 5. The as-prepared CS-DN (a) and the swollen CS-DN (b) were sliced by a blade. The inserts are the hydrogel after slicing resistance test.

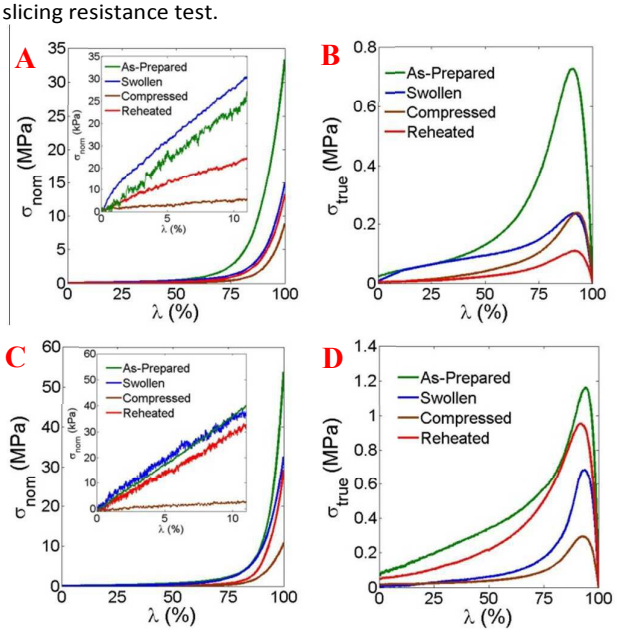

Fig. 6. The stress-strain curves of DN (a) (b) and CS-DN (c)(d).

Table 1. The compressive mechanical properties of DN and CS-DN in different conditions

Sample	Condition	ε_f (%)	σ_f (MPa)	U (kJ/m^2)	E (kPa)
DN	As-prepared	90.5 ±1.9	13.5 ±1.3	2711 ±375	232.2 ±1.1
	Swollen	90.9 ±2.3	5.2 ±0.7	1315 ±150	284.3 ±3.2
	Compressed	93.2 ±1.4	3.5 ±0.5	539 ±58	20.5 ±4.5
	Reheat	91.8 ±1.8	5.1 ±0.6	955 ±119	98.8 ±4.5
CS-DN	As-prepared	94.2 ±1.3	20.4 ±3.8	3544 ±486	321.3 ±1.1
	Swollen	93.6 ±2.2	10.9 ±0.7	1426 ±85	364.7 ±7.2

	Compressed	93.5 ±1.6	4.6 ±0.3	702 ±47	29.8 ±0.5
	Reheat	91.9 ±2.0	12.1 ±2.5	2402 ±138	300.1 ±2.9

The compressions of the DN and CS-DN in different conditions are presented in Fig. 6 and summarized in Table 1. Although the as-prepared DN shows high compressive strength at 13.5 MPa, it reduced to only 5.2 MPa after swelling. As the N1 structure is sacrificed during the 1st compression, 67.3% and 40.1% of strength and toughness remain during the followed 2nd compression in the swollen DN, respectively. After reheating, the compressive strength is recovered to 98.1 % compared to the swollen one. However, the Young's modulus and toughness only recovered to 34.8% and 72.6%, respectively. This is because the agar chains collapsed during compression and they can't be fully extended to its original uniformed density. Compared with DN, the CS-DN shows 31.4% to 137.3% of enhancement in compressive strength at different conditions. Notably, after reheating, the CS-DN shows different properties than the DN. The toughness, compressive strength, and Young's modulus recovered to the similar or better levels of the original swollen CS-DN. These results indicate the CS-SNP inside of the hydrogel extends the agar chains back to uniform dispersion after compression. The SEM images (Figure 6) of swollen, compressed, and reheated DN and CS-BN confirmed that the CS-SNP nanoparticles can efficiently maintain the microstructure of the hydrogel during compression. Compared with swollen DN, the compressed DN exhibits small and dense pores and the reheated DN shows large and loose pores. These different morphologies are the results of unrecoveried and collapsed agar chains. On the other hand, the microstructures of the CS-DN are uniform at all three conditions aided by CS-SNP.

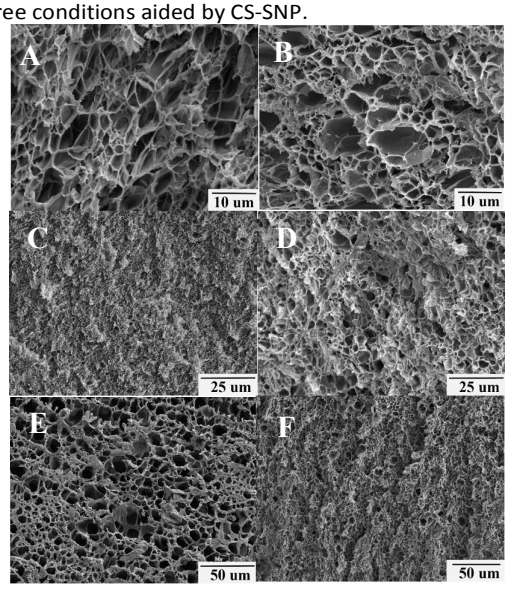

Fig. 7. The SEM of DN and CS-DN in swollen (a)(b), compressed (c)(d), and reheated (e)(f) conditions.

The fatigue resistance of the DN and CS-DN hydrogels was systematically investigated by performing cyclical loading-unloading compressive tests at a constant strain. Fig. 8 presented the consecutive loading-unloading curves with gradient increases in maximum strain on DN and CS-DN. Because of the abrupt of the agar network, the immediate consecutive loading curves with increasing strain almost overlap the previous unloading curves. However, the following CS-DN's curve present an overflow at maximum strain of the previous curve, which is different from the smooth connection of the DN's curves. This phenomenon indicates that the stress of the CS-DN is provided by the agar network as well as the CS-SNP.

The cyclic loading-unloading compressive test further investigates the fatigue resistance of CS-DN systematically. By comparing five cycle loading-unloading compression upon the DN and CS-DN, the importance of the CS-SNP is clearly revealed as presented in Fig. 8 (c) and (d). The hysteresis loop of the DN gel becomes smaller during the cycles. On the other hand, the hysteresis loop of the CS-DN barely changed after the first cycle. These results indicate that after the fracture of the agar network, the CS-DN can still be tough to synergistic dissipate energy by the electrostatic interaction between the CS-SNP and the fractured agar fragments linked with elastic PAA chains while the mechanical properties of DN continuously decay.

The comparison of the hysteresis loops of DN and CS-DN at the fifth loading cycle at different maximum strains (Fig. 8 (e) and (f)) also indicated the significant influencing of the CS-SNP in the fatigue resistance. As summarized by the Table 2. The hysteresis energies of the DN kept decrease with increasing loading cycles. On the other hand, the plateau value of the hysteresis energy of the CS-DN can be found as presented in the Fig. 8(G). Furthermore, the comparisons of the hysteresis energy of the fifth cycle of DN and CS-DN at different maximum strains are presented in Fig. 8(H). The increasing of the E_{hyst} is almost linear dependence on the maximum strain for the DN, while the increasing of E_{hyst} for the CS-DN is likely to be exponential dependence on the maximum strain. In one word, the adding of the CS-SNP significantly reinforced the fatigue resistance of the DN gel. This reinforcing is believed to be the fluid pressurization attributed from the CS-SNP similar like the critical role aggrecan played in the cartilage.

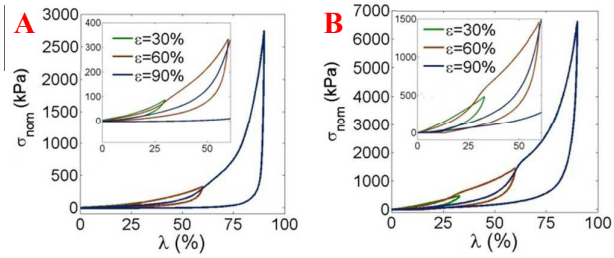

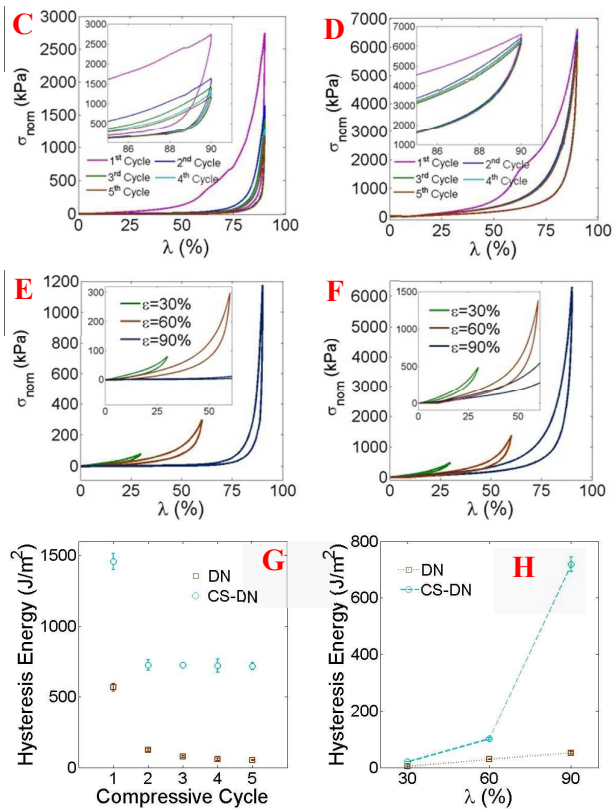

Fig. 8. The typical consecutive loading-unloading curves with gradient increased in maximum strain on the DN (a) and CS-DN (b). Cyclic compressive loading-unloading curves of DN (c) and CS-DN (d) for up to five cycles with 90% maximum strain. The hysteresis loops of DN (e) and CS-DN (f) at the fifth loading cycle at different maximum strains. (g) The hysteresis energies decays with increasing loading cycles at 90% maximum strain. (h) The hysteresis energies of the fifth cycle.

Table 2. The dissipated energy and the maximum stress of hydrogels undergoing cyclic loading with series of predefined maximum strains for 5 cycles.

Sample	No.	30%		60%		90%	
		E_{hyst} kJ/m^2	σ_{max} KPa	E_{hyst} kJ/m^2	σ_{max} KPa	E_{hyst} kJ/m^2	σ_{max} MPa
DN	1	9.1 ±0.5	87 ±2	76.5 ±3.4	333 ±7	568.0 ±27.8	2.7 ±0.6
	2	5.8 ±0.2	83 ±2	34.6 ±1.7	315 ±9	123.8 ±9.8	1.6 ±0.4
	3	5.5 ±0.4	81 ±2	31.4 ±1.9	307 ±4	76.4 ±7.3	1.4 ±0.3
	4	5.3 ±0.3	80.0 ±1	30.0 ±0.7	302 ±8	58.6 ±9.4	1.2 ±0.2
	5	4.4 ±0.2	79.7 ±1	28.9 ±0.4	297 ±8	51.9 ±4.5	1.1 ±0.2
CS-DN	1	58.9 ±1.1	486 ±14	420.8 ±28.5	1433 ±66	1458.3 ±58.4	6.6 ±0.9
	2	26.2 ±1.9	504 ±26	106.8 ±9.8	1435 ±56	725.7 ±38.4	6.4 ±0.8
	3	23.8 ±0.8	494 ±8	112.3 ±9.1	1404 ±30	723.3 ±18.2	6.3 ±0.6
	4	22.0 ±0.7	495 ±6	106.8 ±4.6	1391 ±24	721.3 ±47.7	6.2 ±0.6
	5	20.6 ±0.5	494 ±5	101.2 ±3.9	1391 ±62	717.9 ±25.6	6.2 ±0.7

The internal fracture and fluid pressurization behaviour of the DN and CS-DN were investigated by the swelling experiments of compression-tested gels. All gels were compressed to certain maximum strain before swelling in water. It is found all samples presented slightly increments in swelling ratios as seen in Fig. 9. In the DN gels, the PAA network provides weak osmotic pressure to swell the gel, but restrained by the agar network. When the maximum strains of the compression are small to medium, like 30% to 60%, the agar network remains completed. It can still restrain the PAA. However, after large deformation, like 90% compressive strain, the agar network broke into fragments and the PAA drove the swelling of hydrogel. As a result, the swelling ratios of the DN gels jumped from 37% to 53 % when the maximum strain increased from 60% to 90%, respectively.

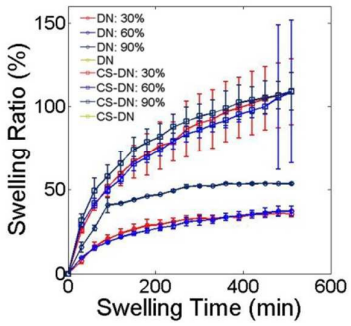

Fig. 9. The swelling of DN and CS-DN hydrogels after 5 cycles of compressive loading-unloading tests at the maximum strains of 30%, 60%, and 90%.

On the other hand, the CS-DN exhibited steady swelling ratio at ~110%. Instead of the weak PAA network, CS-SNP provides strong osmotic pressure. The osmotic pressure is too strong that the agar network cannot restrain it even after small compressive strain, like 30%. Similar like the results of the fatigue resistance, the electrostatic interactions is the major effect to support the CS-SNP after the fracture of the agar network. Although the CS-DN exhibited ~110% swelling ratio during the swelling, its swelling is extremely small compared with other tough hydrogels which are at least 630% [35]. Meanwhile, similar swelling processes are observed on the gels with different maximum strains which indicate the swelling is not dependent on the agar structure. This mechanism of CS-SNP supporting DN gel is similar like the aggrecan plays in the natural cartilage as it provides its osmotic pressure to withstand compression while the collagen network of the cartilage immobilizes the imbibed fluid.

In order to extend the service time of the hydrogel, the mechanical properties need to be fully recoverable due to the complicated daily activities. Fig. 10 presented the compressive results during cyclical heating. Although the compressive

strengths are similar as the original, the toughness of the swollen DN decreases after recovery. On the other hand, both the compressive strengths and the toughness of CS-DN recovered to their original states. This is because CS-SNP entangled with agar chains and extended them to uniform density after the compression. The heating treatment improves the entanglement between CS-SNP and the agar chains by trapping CS-SNP with helix agar chains. The agar chains in the DN, on the other hand, can be only dragged partially to its original density when the PAA network recovery the hydrogel shape after the compression. In that case, the CS-DN presents fully self-recoverable mechanism with the help of the CS-SNP.

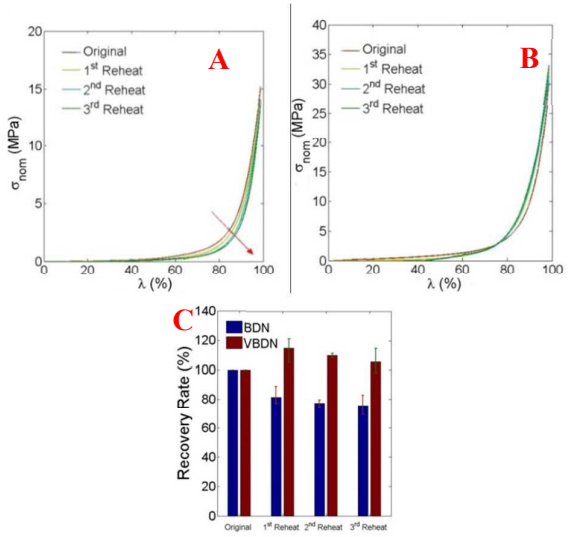

Fig. 10. The mechanical recovery of DN (a) and CS-DN (b); (c) The comparison of their toughness recovery rate.

5 Conclusions

In this work, a hydrogel with high toughness, strong fatigue resistance, and fully recoverable mechanical properties was fabricated. The highly charged CS-SNP, bio-inspired from aggrecan, is synthesized to extend the agar chains. The osmotic properties provided by the CS-SNP not only increase the modulus and strength of hydrogel, but also maintain its microstructure as proved by the SEM images. The cyclic compression test and the swelling test indicated a significant improving on the fatigue resistance after adding CS-SNP. The cyclic compress/heating test proved that the strength and toughness can be fully recovered with the aid of CS-SNP. In one word, the agar/PAA is tough, fatigue resistant, and fully recoverable enhanced by CS-SNP. This hydrogel is the promising material for the long-term application with high mechanical properties for both daily use and extreme conditions.

Acknowledgement

The authors would like to acknowledge the supporting from NSF grant (#: 1228127). The authors would like the thank Imaging Centre of Texas Tech University for the help of freeze drying, TEM and SEM.

Reference:

1. T. R. Hoare and D. S. Kohane, *Polymer*, 2008, **49**, 1993-2007.
2. M. Kobayashi, Y. S. Chang and M. Oka, *Biomaterials*, 2005, **26**, 3243-3248.
3. V. Chan, K. Park, M. B. Collens, H. Kong, T. A. Saif and R. Bashir, *Sci Rep-Uk*, 2012, **2**.
4. J. A. Burdick and W. L. Murphy, *Nat Commun*, 2012, **3**.
5. A. Skardal, D. Mack, E. Kapetanovic, A. Atala, J. D. Jackson, J. Yoo and S. Soker, *Stem Cell Transl Med*, 2012, **1**, 792-802.
6. S. Michael, H. Sorg, C. T. Peck, L. Koch, A. Deiwick, B. Chichkov, P. M. Vogt and K. Reimers, *Plos One*, 2013, **8**.
7. J. Y. Sun, X. H. Zhao, W. R. K. Illeperuma, O. Chaudhuri, K. H. Oh, D. J. Mooney, J. J. Vlassak and Z. G. Suo, *Nature*, 2012, **489**, 133-136.
8. C. W. Peak, J. J. Wilker and G. Schmidt, *Colloid Polym Sci*, 2013, **291**, 2031-2047.
9. T. Nakajima, T. Kurokawa, H. Furukawa, Q. M. Yu, Y. Tanaka, Y. Osada and J. P. Gong, *Chinese J Polym Sci*, 2009, **27**, 1-9.
10. J. P. Gong, Y. Katsuyama, T. Kurokawa and Y. Osada, *Advanced Materials*, 2003, **15**, 1155-+.
11. Y. H. Na, T. Kurokawa, Y. Katsuyama, H. Tsukeshiba, J. P. Gong, Y. Osada, S. Okabe, T. Karino and M. Shibayama, *Macromolecules*, 2004, **37**, 5370-5374.
12. T. Nakajima, H. Furukawa, Y. Tanaka, T. Kurokawa, Y. Osada and J. P. Gong, *Macromolecules*, 2009, **42**, 2184-2189.
13. Y. H. Na, *Korea-Aust Rheol J*, 2013, **25**, 185-196.
14. Q. Chen, L. Zhu, C. Zhao, Q. M. Wang and J. Zheng, *Advanced Materials*, 2013, **25**, 4171-4176.
15. A. Nakayama, A. Kakugo, J. P. Gong, Y. Osada, M. Takai, T. Erata and S. Kawano, *Adv Funct Mater*, 2004, **14**, 1124-1128.
16. H. H. Shin, B. D. Olsen and A. Khademhosseini, *J Mater Chem B*, 2014, **2**, 2508-2516.
17. Q. Chen, L. Zhu, H. Chen, H. L. Yan, L. N. Huang, J. Yang and J. Zheng, *Adv Funct Mater*, 2015, **25**, 1598-1607.
18. J. P. Gong, *Soft Matter*, 2010, **6**, 2583-2590.
19. W. Yang, H. Furukawa and J. P. Gong, *Advanced Materials*, 2008, **20**, 4499-4503.
20. S. E. Bakarich, G. C. Pidcock, P. Balding, L. Stevens, P. Calvert and M. I. H. Panhuis, *Soft Matter*, 2012, **8**, 9985-9988.
21. X. Lu, C. Y. Chan, K. I. Lee, P. F. Ng, B. Fei, J. H. Xina and J. Fub, *J Mater Chem B*, 2014, **2**, 7631-7638.
22. C. Kiani, L. Chen, Y. J. Wu, A. J. Yee and B. B. Yang, *Cell Res*, 2002, **12**, 19-32.
23. P. J. Roughley and J. S. Mort, *Journal of Experimental Orthopaedics*, 2014, **1**.
24. Y. Zhao, T. Nakajima, J. J. Yang, T. Kurokawa, J. Liu, J. Lu, S. Mizumoto, K. Sugahara, N. Kitamura, K. Yasuda, A. U. D. Daniels and J. P. Gong, *Advanced Materials*, 2014, **26**, 436-442.

25. J. C. Bernhard and A. Panitch, *Acta Biomater*, 2012, **8**, 1543-1550.
26. S. Sarkar, S. E. Lightfoot-Vidal, C. L. Schauer, E. Vresilovic and M. Marcolongo, *Carbohydr Polym*, 2012, **90**, 431-440.
27. G. T. Hermanson, *Bioconjugate Techniques*, Academic Press, 2013.
28. M. Marini, B. Pourabbas, F. Pilati and P. Fabbri, *Colloid Surface A*, 2008, **317**, 473-481.
29. U. Gulyuz and O. Okay, *Macromolecules*, 2014, **47**, 6889-6899.
30. M. Foot and M. Mulholland, *J Pharm Biomed Anal*, 2005, **38**, 397-407.
31. F. Cabassi, B. Casu and A. S. Perlin, *Carbohydrate Research*, 1978, **63**, 1-11.
32. J. M. Huang, H. J. Huang, Y. X. Wang, W. Y. Chen and F. C. Chang, *J Polym Sci Pol Phys*, 2009, **47**, 1927-1934.
33. Q. Wang, R. X. Hou, Y. J. Cheng and J. Fu, *Soft Matter*, 2012, **8**, 6048-6056.
34. R. Tao and S. L. Simon, *J Polym Sci Pol Phys*, 2015, **53**, 621-632.
35. G. L. Du, G. R. Gao, R. X. Hou, Y. J. Cheng, T. Chen, J. Fu and B. Fei, *Chem Mater*, 2014, **26**, 3522-3529.

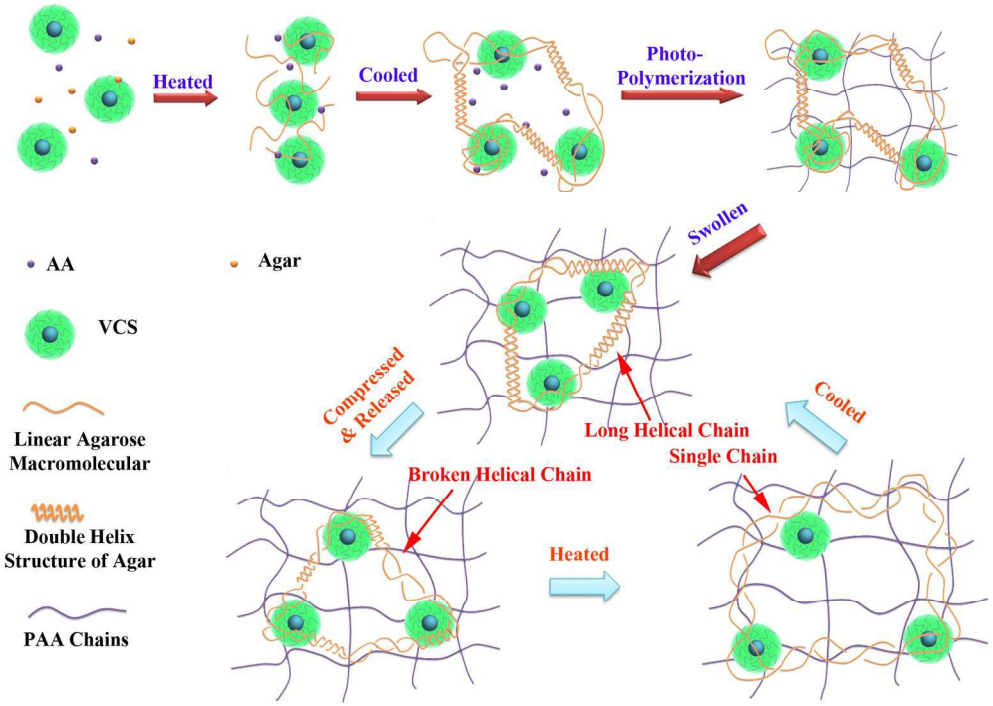

177x127mm (300 x 300 DPI)